Simulation of air transformers with different sizes and geometry

Dimcho Hvarchilkov
Department of Power Electronics
Technical University of Sofia
Bulgaria
hvarchilkov@gmail.com

Vladimir Dimitrov
Department of Power Electronics
Technical University of Sofia
Bulgaria
vdimitrov88@gmail.com

Peter Goranov
Department of Power Electronics
Technical University of Sofia
Bulgaria
pgoranov@ecad.tu-sofia.bg

I. INTRODUCTION

Nowadays wireless power transfer (WPT) systems are becoming more popular in many areas of electronics. In those kind of systems there is no wire connection between a power source and a load [1]. Consequently, there is no need of power connectors, which additionally reduces the probability of malfunction. WPT systems are used for many purposes such as charging a smartphone or an electrical toothbrush at home, charging an electrical vehicle and many others. It is very useful for powering hermetically sealed devices, such as devices used in space or medical equipment [2][3]. Moreover, it allows power transfer to constantly moving parts in industrial and space equipment, without wires. Amongst the classes of wireless systems, inductive energy transfer systems have been widely studied, due to their high efficiency and high transmission power capability [4].

In inductive coupled systems, an inverter supplies alternative current to the primary coil, which produces a magnetic field at the secondary coil. The produced field induces a voltage across the secondary coil, which can be rectified and supplied to a load. An important parameter for inductive link is the coupling coefficient k, which measures how much power from the generated electromagnetic (EM) field is induced in the secondary coil [1]. Owing to this, the coupling coefficient is directly related to the system efficiency and the operation mode of the inverter.

Previous studies show that the coupling coefficient depends mostly on the gap between the transmitting and the receiving coils, the relative angle between the coils, the displacement of the geometrical centers of the coils and the magnetic properties of the material surrounding the coils [5][6]. These four variables make the analysis very complex, especially in some cases. An example is a system with coils of different geometry, such as round and square, and a displacement between the geometric centers of the coils. Another example could be a system with nonlinear magnetic permeability of the materials surrounding the coils, such as a transition between different types of magnetic core. Of course, the most complex case would be a combination of all options, which is usually the practical case.

Analytical approaches to determining the coupling coefficient are flawless when there is a well-defined problem. In this case, they can provide fast solutions and acceptable accuracy of the result. In complex problems, analytical methods are difficult to solve without some simplifications. As a result, the accuracy decreases. Besides this, there are some complex situations where analytical methods are nearly inapplicable.

On the other hand, numerical simulations, based on finite element analysis (FEA), provide highly accurate results and the possibility of solving very complex problems. Unfortunately, FEA requires long computational time and extensive memory usage. On account of this, the simulation model should be well designed and optimized.

In this paper, FEA simulation will be done for several coils with different sizes and geometry. The environment, which will be used for the simulations, is "ANSYS® – Electronics desktop". The package for direct current and low frequency electromagnetic simulations is called "Maxwell®". In the second chapter, the simulation design is described, and all the parameters are set. In the third and fourth chapter, the results of the simulation are presented, and its comparison to a real system is discussed.

II. DESCRIPTION OF THE SIMULATION DESIGN

A. Sizes and geometry of the coils

Various types of coil geometry are chosen for the transmitting and the receiving coils. The main idea is to determine which type of geometry has the best coupling coefficient and how the size of the coils affects it.

All coils are wound with flat copper wire with a size of 1mm x 10mm (width x height).

- Two equal circular coils with large diameter (210mm).
- Two equal circular coils with small diameter (800mm).
- Two circular coils with different diameters (220mm and 310mm).
- Two equal square coils with the same size as the small circular coils. Side length is 210mm.
- Two equal spiral coils with diameter 210mm.
- Two equal rectangular coils with dimensions a x b (330mm x 160mm).
- One rectangular coil with a size of a x b (330mm x 160mm) and one circular with diameter (210mm).

B. *Simulation conditions and variables*

Satisfying results can be achieved, if the simulation conditions are well defined. First of all, some of the parameters have to be static. They do not vary through the simulation process.

- The inductance (L) of all tested coils is nearly equal and is around 16μH. This value is chosen based on an existing actual model.
- The space around the coils is pure air, which means that the distribution medium is isotropic. Hence, the magnetic permeability is equal in all partitions of the volume.
- The current through the coils is equal in all simulations and has value of 10Amps.
- The transmitting coil is fixed, while the receiving coil is movable.

Secondly, the variables have to be specified. These are the parameters which are varied during the optimization process. The illustration shown on Fig. 1 gives clarity on these parameters.

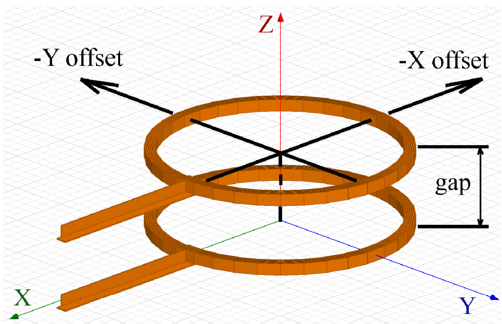

Fig. 1 – The variable parameters: offset - *X*, *Y* and the gap - *Z*.

- The gap between the coils varies from $Z_{min} = 25$mm to $Z_{max} = 200$mm, with step size $S = 25$mm.
- The relative disposition (X or/and Y) between the geometric centers is varied on every step on the gap change. The disposition varies from 0mm (the geometric centers match) to 150mm and the step size is 50mm.
- The size of the simulation region is fixed for every particular coil set. Its size is at least 60% larger than the tested coil dimension in all directions. If the region is smaller, lack of accuracy will be presented. Example of the region is shown on Fig. 2.

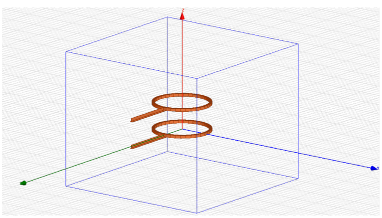

Fig. 2 – Simulation region of one of the tested coil set.

III. Calculation of Self Inductance of Circular Coils

The inductance of all coils should be calculated roughly before the simulations, due to their modeling. Formulae designed for inductance calculation for ideal solenoids are feasible only when the length of the coil is much longer than its diameter. Owing to this, the modified formula (1) will be used.

$$L = \frac{N\Phi}{I} = \frac{NAB_z}{I} =$$

$$= 2\frac{NA}{I}\frac{\mu NI}{2l}\left[\frac{(l/2)-l}{\sqrt{(l-l/2)^2+R^2}} + \frac{(l/2)+l}{\sqrt{(l+l/2)+R^2}}\right] = \tag{1}$$

$$= \frac{N^2\pi R^2\mu}{l}\left[\frac{(l/2)-l}{\sqrt{(l-l/2)^2+R^2}} + \frac{(l/2)+l}{\sqrt{(l+l/2)^2+R^2}}\right]$$

Where: N – number of turns, $\Phi = B_z A$ – magnetic flux, A – area of the coil, μ – permeability of air, B – magnetic induction through the area enclosed by the coil, l – the coil's length, R – the coil radius, B_z – magnetic induction in finite length solenoid.

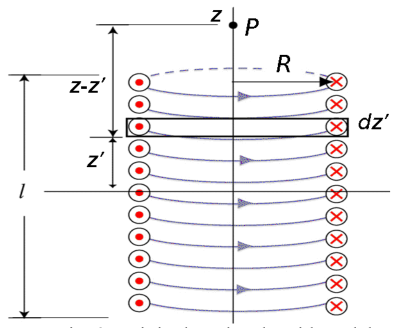

Fig. 3 – Finite length solenoid model

The magnetic field in a finite length solenoid is not uniform, therefore it must be calculated in advance. Equation (2) expresses B_z and Fig. 3 shows the model of a short solenoid [8]. Equation [8](1) must be multiplied by two, owing to the magnetic induction B_z being given only for the half part of the coil at point "P" with coordinates "z". The coordinate "z" becomes same as the length "l" in equation (1) on account of the magnetic field at point "P" decreases significantly when ($z > l$).

$$B_z = \frac{\mu NIR^2}{2l}\int_{-\frac{l}{2}}^{+\frac{l}{2}} \frac{dz'}{[(z-z')^2+R^2]^{\frac{2}{3}}} =$$

$$= \frac{\mu NIR^2}{2l}\frac{z'-z}{R^2\sqrt{(z-z')^2+R^2}}\Bigg|_{-\frac{l}{2}}^{+\frac{l}{2}} = \tag{2}$$

$$= \frac{\mu NI}{2l}\left[\frac{(l/2)-z}{\sqrt{(z-l/2)^2+R^2}} + \frac{(l/2)+z}{\sqrt{(z+l/2)^2+R^2}}\right]$$

IV. SIMULATIONS RESULTS AND PRACTICAL COMPARISON

The transmission coils are labeled LTx and the receiving coils are labeled LRx. In all sections below, the results are shown in tables and charts. At the beginning of each section, a 3D view of the particular analyzed subject is given.

For coils that are rotationally symmetrical, such as the circular and the square, the offset should be varied in one direction only (*X* or *Y*). Due to the offset in *X*-direction changing the length of the coil leads, it is better that *Y*-direction be chosen for the study. One chart per experiment is needed in this case. However, when one or both coils are not rotationally symmetrical, as the rectangular, the offset should be varied in both directions (*X* and *Y*). Consequently, more than one chart will be necessary for these instances.

A. Two equal circular coils with small diameter $D_S \approx 210mm$.

In this first section, a comparison between real measured, analytically calculated and simulation data is made. All dimensions and geometry are nearly equal. The numbers of turns is 6 for all coils in this section.

Results about the self-induction are shown in Table 1. The coupling coefficient data is listed in Table 2 and is graphically illustrated with the chart on Fig. 5. The “Experimental” curve shows the result from the practical measurement and it is done without any offset, namely $X=Y=0mm$.

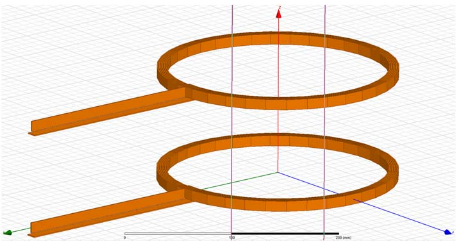

Fig. 4 – 3D view of 2 x 220mm circular coils.

Table 1 – Parameters of 2 x 220mm cirlular coil set.

	D, mm	N	Lcalc, μH	Lsim, μH	Lx, μH
LTx	220	6	15.62	15.29	14.39
LRx	220	6	15.62	15.29	14.39

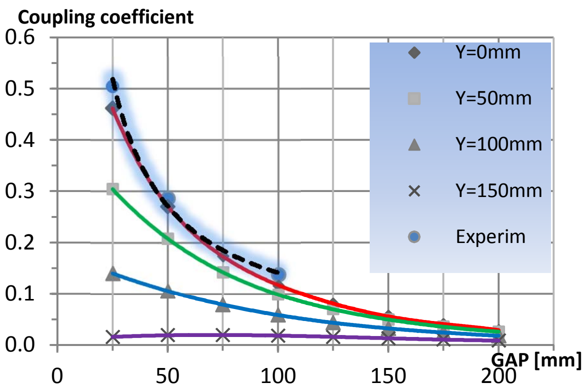

Fig. 5 – Coupling coefficient (2x220mm circular coils).

The self-induction is measured with a resonant method using parallel R-C circuit and measuring the voltage across it. The experimental stand is shown on Fig. 6 and its schematic diagram – on Fig. 7. The equation used for calculating the coil’s self-induction is (3) and its resulting value (L_x) is listed in Table 1. Measurement is done in two steps. Firstly, the inductance L_1 (Fig. 9) is measured with the switch (sw) open. Secondly, L_1 is measured again with the switch closed, which shortens the L_2. As a result, L_1 decreases its value to (L_s). The coupling coefficient is calculated using equation (4)[8].

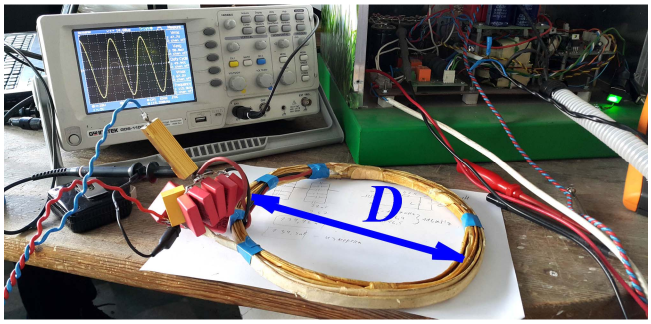

Fig. 6 – The experimental stand for measuring self-induction - L_x.

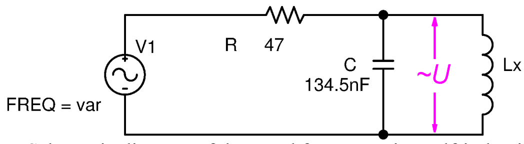

Fig. 7 – Schematic diagram of the stand for measuring self-induction - L_x.

$$L_x = \frac{1}{4\pi^2 f_0^2 C} = \frac{1}{4\pi^2 114400^2 \cdot 135.4 \cdot 10^{-9}} = \\ = 14.39\mu H \qquad (3)$$

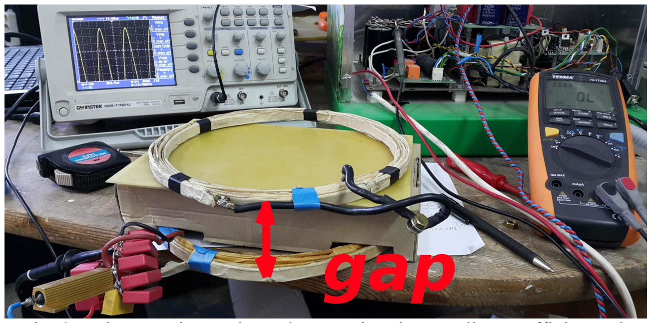

Fig. 8 – The experimental stand measuring the coupling coefficient – *k*.

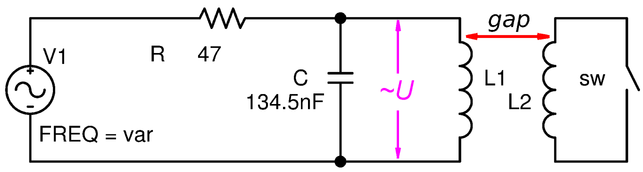

Fig. 9 – Schematic diagram of the stand measuring the coupling coefficient.

$$k = \sqrt{\left(1 - \frac{L_S}{L_1}\right)} \qquad (4)$$

Table 2 – Data from the practical measurement of the coupling coefficient.

Gap \	L_1, μH	L_S, μH	k
25	14.128	10.528	0.504
50	14.376	13.198	0.286
100	14.401	14.128	0.137

B. Two equal circular coils with large diameter $D_L \approx 800mm$.

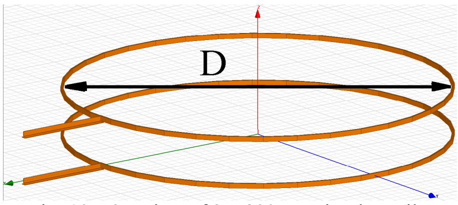

Fig. 10 – 3D view of 2 x 800mm circular coils.

	D, mm	N	Lcalc, μH	Lsim, μH
LTx	808	3	14.35	19.85
LRx	808	3	14.35	19.85

Table 3 – Parameters of 2 x 800mm cirlular coil set.

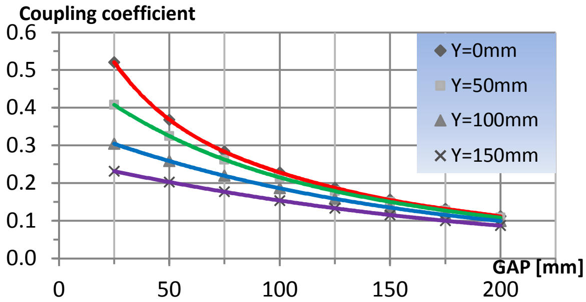

Fig. 11 – Coupling coefficient (2 x 800mm circular coils).

C. Two circular coils with different diameters $D_S \approx 220mm$ and $D_M \approx 320mm$.

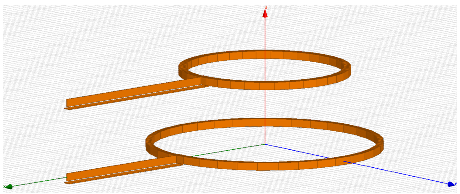

Fig. 12 – 3D view of 310mm and 220mm circle coils.

Table 4 – Parameters of 310mm and 220mm circle coil set.

	D, mm	N	Lcalc, μH	Lsim, μH
LTx	310	5	15.29	17.66
LRx	220	6	15.62	16.23

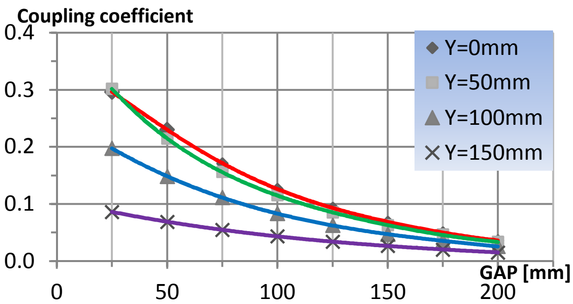

Fig. 13 – Coupling coefficient (310mm and 220mm circle coils).

D. Two equal square coils with the same size as the circular diameter DS. Side length is A = 210mm.

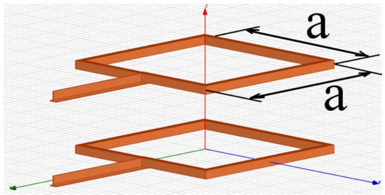

Fig. 14 - 3D view of 2 x 220mm square coils.

Table 5 – Parameters of 2 x 220mm square coil set.

	a, mm	N	Lcalc, μH	Lsim, μH
LTx	220	6	16.48	18.14
LRx	220	6	16.48	18.14

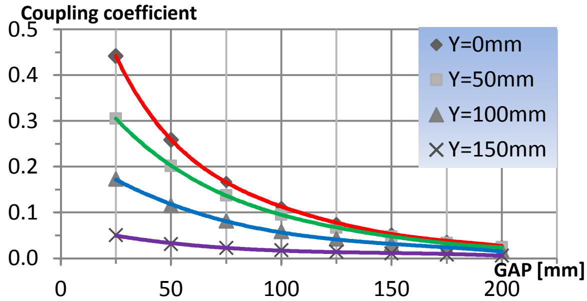

Fig. 15 – Coupling coefficient (2 x 220mm square coils).

E. Two circular flat spiral coils with diameter 210mm.

The equation (1) is not suitable for calculating self-inductance in the case of spiral coils. Instead, modified Wheeler's formula (5) for planar spiral coil will be used [9].

$$L_{wm} = \frac{K_1 \mu N^2 D_{avg}}{1 + K_2 \rho}, \qquad where\ \rho = \frac{D_{max} - D_{min}}{D_{max} + D_{min}}, \qquad (5)$$

$D_{avg} = 0.5(D_{max} + D_{min})$, $K_1=2.25$, $K_2=3.55$. The coefficients are given for octagonal planar coil, which yields error under 5%.

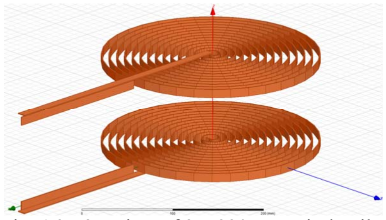

Fig. 16 – 3D view of 2 x 220mm spiral coils.

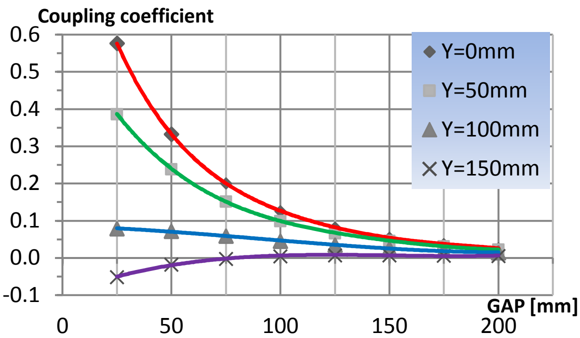

Figure 17 – Coupling coefficient for 2 x 220mm spiral coils.

Table 6 – Parameters of 2 x 220mm spiral coil set.

	D, mm	N	Lcalc, μH	Lsim, μH
LTx	205	14	14.81	14.82
LRx	205	14	14.81	14.82

F. Two equal rectangular coils with dimensions A x B (B ≈ 330mm and C ≈ 160mm).

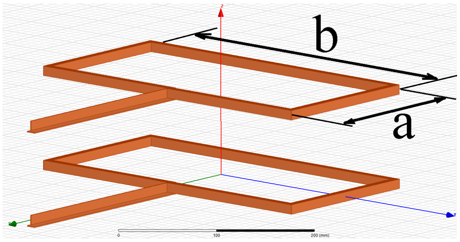

Fig. 18 – 3D view of two equal rectangular coils (330 x 160)mm.

Table 7 – Parameters of coil set (rectangular 2 x 330 x 160mm).

	a, mm	b, mm	N	Lcalc, μH	Lsim, μH
LTx	160	330	5	13.5	16.2
LRx	160	330	5	13.5	16.2

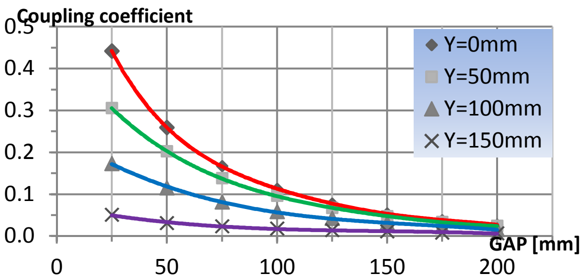

Fig. 19 – Coupling coefficient for two equal rectangular coils (330x160)mm, X-offset = 0mm, Y-offset varies.

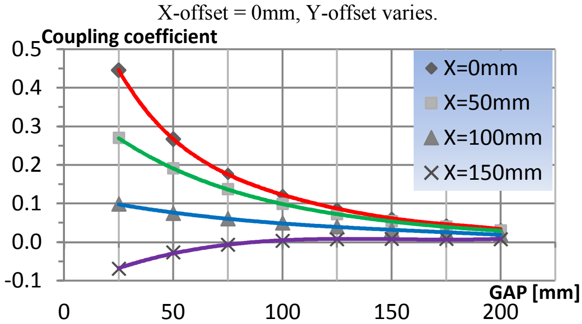

Fig. 20 – Coupling coefficient for two equal rectangular coils (330 x 160)mm, X - offset varies, Y - offset = 0mm.

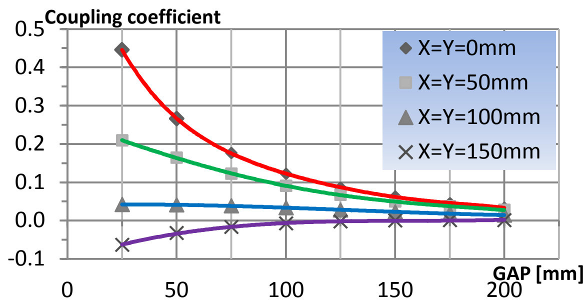

Fig. 21 – Coupling coefficient for two equal rectangular coils (330 x 160)mm, X=Y – offsets both vary.

G. One rectangular coil with a size of a x b (330mm x 160mm) and one circular with diameter (220mm).

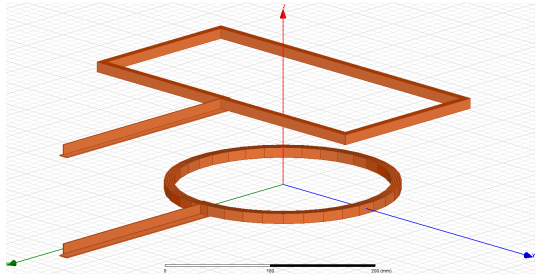

Fig. 22 – 3D view of a rectangular coil and a circular coil.

Table 8 – Parameters of rectangular and circular coils.

	D, a, mm	b, mm	N	Lcalc, μH	Lsim, μH
LTx	220	-	6	15.62	16.32
LRx	160	330	5	13.53	16.1

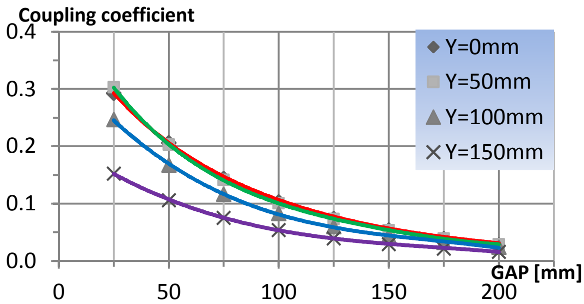

Fig. 23 – Coupling coefficient for rectangular and circular coils, X-offset = 0mm, Y-offset varies.

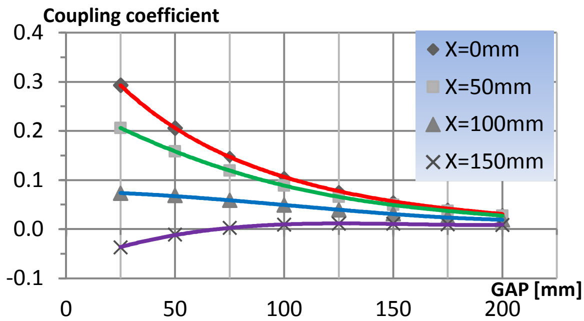

Fig. 24 – Coupling coefficient for rectangular and circular coils X-offset varies, Y-offset = 0mm.

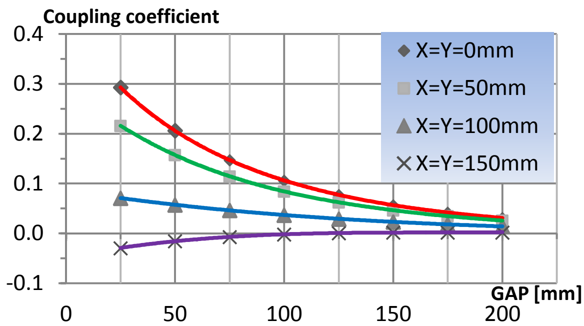

Fig. 25 – Coupling coefficient for rectangular and circular coils X=Y – offsets both vary.

V. CONCLUSION

In the third chapter, an equation for rough inductance calculation of a short length circular coil is proposed. The deviation from the real value depends on the diameter to length ratio *(D / l)*. The error is below 3% when *(D / l = 21)* – Table 1, and it is around 28% when *(D / l = 80)* – Table 3. The equation can be used, but the error must be considered.

All the results in chapter IV show correlation between the simulated results, those taken from the real measurement and the theoretically calculated. In section A, the coupling coefficient is measured using a real model and the results are displayed in charts and tables. Additionally, the inductance of the coils is measured practically too. In all sections in chapter IV the inductance of all simulated coils is analytically computed and compared with the simulated values.

All the examined coils have different properties.

The results for the *two equal coil set with small diameter* (210mm, Fig. 4) shows that the coupling coefficient has intermediate value amongst the other tested coil sets. The offset changes the coupling coefficient significantly, thus this version of the coil set imposes high accuracy about the positioning.

The *large (800mm), circular coil set* (Fig. 10) has good coupling coefficient and the offset has poor influence as compared to all others. But it needs extra space and longer wire.

The *two different circular coil set* (Fig. 12) has relatively lower coupling coefficient, but small offsets mostly do not affect it. This option is suitable in cases where the positioning is often inaccurate.

The *small square coil set* (220mm - Fig. 14) presents results that are nearly identical to the *two equal coil set with small diameter*. The difference is that the coupling coefficient decreases less than that of the *circular coil set*, for the same values of the offset.

The coupling coefficient reaches its maximum value with the *spiral circular coil set* (Fig. 16), but only for short gaps. When the gap is around 100mm the coupling coefficient has a value close to the *rectangular* and the *circular coil sets*. An interesting result in this case is that phase shifting is present when the offset is 150mm. Consequently, the k will be zero at some point between 100mm and 150mm offset.

The results of the *rectangular coil set* (Fig. 18) display that the coupling coefficient (k) behaves similarly to that of the *small circular* and *square coil sets* in case of offset in Y-direction only. If X-offset is applied, k decreases progressively and a phase shift appears at X-offset=150mm.

The *set of a rectangular coil* and a *circular coil* has similar properties to the *rectangular coil set*, but with a few differences. The coupling coefficient's maximum is about 33% less than the *rectangular coil set*; nevertheless, at 100mm gap, the values are nearly the same. Offsets under 50mm in Y-direction do not affect k. Moreover, Y-offset has weaker influence on k as compared to *rectangular coil set*. Offsets in X-direction decrease k faster than the *rectangular set*, and again, phase shift is present at 150mm X-offset. This type of coil set can be used when positioning accuracy is low.

The results of the analysis could help with selecting the most appropriate coil properties for a given scenario. The proposed method could save time and funds during the design of the coils and prototypes.

REFERENCES

[1] Rafael Mendes Duarte, Gordana Klaric Felic, "Analysis of the Coupling Coefficient in Inductive Energy Transfer Systems", Active and Passive Electronic Components Volume 2014, Article ID 951624, 6 pages ,17 June 2014.

[2] Gabriel Vazquez Ramos, Jiann-Shiun Yuan, "Wireless Power Transfer for Apace Applications", NASA Kennedy Space Center; Cocoa Beach, FL, United States.

[3] Pyungwoo Yeon, S. Abdollah Mirbozorgi, Bruce Ash, Helmut Eckhardt,Maysam Ghovanloo, "Fabrication and Microassembly of a mm-Sized Floating Probe for a DistributedWireless Neural Interface", 1 September 2016, Georgia Institute of Technology, Atlanta, GA 30308, USA.

[4] A. Kurs, A. Karalis, R. Moffatt, J. D. Joannopoulos, P. Fisher, M. Soljaˇci´c, "Wireless power transfer via strongly coupled magnetic resonances," Science, vol. 317, no. 5834, pp. 83–86, 2007.

[5] Ki-Bong Kim, Zivan Zabar, Senior Member, Leo Birenbaum,"Mutual Inductance of Noncoaxial Circular Coils with Constant Current Density", IEEE transactions on magnetics, vol. 33, no. 5, pages 4303-4309, seetember 1997.

[6] Vissuta Jiwariyavej, Takehiro Imura, Yoichi Hori, "Coupling Coefficients Estimation of Wireless Power Transfer System via Magnetic Resonance Coupling using Information from Either Side of the System", University of Tokyo, Japan.

[7] Sen-ben Liao, Peter Dourmashkin, John Belcher - MIT, "Physics 8.02 Electricity and Magnetism", Chapter 9 – "Sources of Magnetic field", p9, p20 – p23.

[8] G. Barrere – Exality Corporation, "Measuring Transformer Coupling Factor k".

[9] Sunderarajan S. Mohan, Maria del Mar Hershenson, Stephen P. Boyd, and Thomas H. Lee, "Simple Accurate Expressions for Planar Spiral Inductances", IEEE Journal Of Solid-State Circuits, Vol. 34, No. 10, October 1999, p1419-p1421.